RAPID COMMUNICATIONS

PHYSICAL REVIEW B VOLUME 43, NUMBER 10 1 APRIL 1991

Electronic and structural effects of oxygen doping in $Bi_2Sr_2CaCu_2O_x$ superconductors characterized by tunneling microscopy

Xian Liang Wu, Yue Li Wang, Zhe Zhang, and Charles M. Lieber
Department of Chemistry, Columbia University, New York, New York 10027
(Received 19 December 1990)

Scanning tunneling microscopy has been used to characterize the electronic and structural effects of oxygen doping in $Bi_2Sr_2CaCu_2O_x$ materials. Bias-voltage-dependent images of oxygen-deficient nonsuperconducting crystals show that reversible oxygen loss leads to nonperiodic variations in the electronic states near the Fermi level (± 300 mV). Variations in the electronic states near the Fermi level are not observed, however, in images of superconducting samples. In addition, high-resolution images of the BiO layer of oxygen-deficient samples do not exhibit vacancies or strongly perturbed sites, but rather appear similar to images of the BiO layer of superconducting crystals. These data indicate that suppression of T_c in $Bi_2Sr_2CaCu_2O_x$ may not be due to oxygen loss from the BiO layer.

It is widely recognized that oxygen doping plays a key role in determining the properties of copper oxide superconductors.[1-6] For example, the results from many studies have established that variations in oxygen concentration change the average carrier concentration and thereby T_c. More striking are recent observations suggesting that subtle oxygen rearrangements can lead to superconductivity and enhanced fractions of superconducting material even when the average oxygen stoichiometry remains constant.[3-6] To understand these and other important effects it is essential to characterize variations in the microstructure and the local electronic structure associated with oxygen doping. Determination of the local structure including oxygen-atom positions by diffraction techniques is inherently difficult due to crystal disorder and the small scattering cross section of oxygen.[7,8] Recent neutron-diffraction studies have, however, provided insight into important oxygen positional variations in $YBa_2Cu_3O_{7-x}$ as a function of x and time.[3,4]

In the $Bi_2Sr_2CaCu_2O_x$ materials the variation of T_c with oxygen stoichiometry has been investigated by several groups.[9-15] Studies of single-crystal materials have shown that T_c can be suppressed by annealing in low-oxygen partial pressures.[9-11] To date, changes in the microstructure associated with such oxygen doping have not been addressed. Neutron- and x-ray-diffraction studies of the parent compound have suggested that extra oxygen is incorporated into the BiO layer of this material,[7,8] and it has been assumed[7-9,12-15] that variations in the oxygen stoichiometry responsible for changes in T_c occur in this layer. Spatial variations in the electronic properties due to oxygen doping, which may be especially important in these short-coherence-length materials,[6] have not yet been characterized in either $Bi_2Sr_2CaCu_2O_x$ or $YBa_2Cu_3O_{7-x}$.

Herein we apply a different approach, scanning tunneling microscopy (STM), to characterize the local electronic and structural effects of oxygen doping in $Bi_2Sr_2CaCu_2O_x$ crystals. Bias-voltage-dependent STM images of the BiO layer of oxygen-deficient nonsuperconducting crystals show that oxygen loss leads to spatial variations in the electronic states near the Fermi level which are not observed in images of the superconducting ($T_c \approx 85$ K) samples. These variations in the electronic states can be removed by annealing the oxygen-deficient samples in air; this latter anneal yields materials that are superconducting with $T_c \approx 85$ K. In addition, atomic resolution images of the BiO layer structure are similar for both the oxygen deficient and superconducting samples, and thus these data indicate that the observed changes in T_c may not be due to oxygen loss from the BiO layer. Although we have been unable to characterize structural variations due to oxygen loss, these results demonstrate that the local electronic effects of oxygen doping can be mapped out by STM.

Single crystals of $Bi_2Sr_2CaCu_2O_x$ were grown from CuO-rich melts.[10,16] Oxygen was removed from as-grown superconducting crystals ($T_c \approx 85$ K) by vacuum annealing ($P = 10^{-3}$ Torr) at 400 °C. We find that these conditions yield systematic decreases in T_c as a function of annealing time.[10] Typically, T_c decreases to ≈ 50 K after 3 h and the samples become nonsuperconducting after 30 h, as shown in Fig. 1. Resistivity measurements made on the nonsuperconducting crystals demonstrate that these materials are semiconducting down to 4.2 K. The suppression of superconductivity through vacuum annealing is also reversible; that is, annealing nonsuperconducting crystals in air at 400 °C for > 8 h yields $T_c = 85$-K superconducting material (Fig. 1). Thermogravimetric analyses of our crystals show that these changes in T_c (85 K to semiconductor) are related to a reversible 2.5–3.0% change in the oxygen concentration.

Our STM measurements were made with a modified commercial instrument (Nanoscope, Digital Instruments, Inc.) operated in an argon-filled glove box equipped with a purification system that reduced the concentrations of H_2O and O_2 below 1 ppm.[17] Reproducible and stable (≥ 6 h) STM measurements were obtained for samples cleaved *in situ*. As discussed previously, single crystals of the quasi-two-dimensional superconductor $Bi_2Sr_2CaCu_2O_x$ cleave preferentially along the weakly interacting

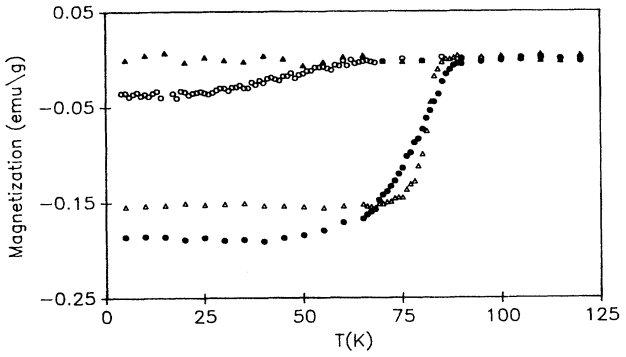

FIG. 1. Magnetization vs temperature data for $T_c = 85$-K (●), $T_c \approx 60$-K (○), and nonsuperconducting (▲) samples recorded using a superconducting quantum interference device magnetometer (MPMS, Quantum Design); the samples were cooled in a field of 5 Oe from 298 K. The $T_c \approx 60$-K sample was prepared by annealing at 400 °C in vacuum for 2.5 h and the nonsuperconducting sample was prepared by annealing in vacuum for 30 h. Reannealing the nonsuperconducting sample at 400 °C in air for 9 h restores the superconducting properties as shown (△).

BiO/BiO double layers to yield a BiO surface that is structurally similar to the bulk.[10,18,19] Photoemission[20,21] and high-resolution electron energy loss[22] studies of cleaved $Bi_2Sr_2CaCu_2O_x$ surfaces have also detected an energy gap below the bulk T_c which indicates that the surface region is superconducting. It is thus reasonable to assume that surface-sensitive experiments such as STM have bearing on understanding superconductivity in $Bi_2Sr_2CaCu_2O_x$. In addition, direct studies of the BiO layer by STM are especially attractive since extra oxygen in this layer has been proposed to affect the carrier concentration and to cause the one-dimensional superstructure in this material.[7,9,12–15,23,24]

Gray-scale images of the BiO layer for $T_c = 85$-K materials and nonsuperconducting $Bi_2Sr_2CaCu_2O_x$ crystals are shown in Fig. 2. These data are typical of the > 50 images obtained on at least ten independent samples and thus we believe they are representative of the intrinsic properties of the oxygen-doped materials. The images of the $T_c = 85$-K materials and the high bias-voltage (V_b) images of nonsuperconducting crystals both exhibit the one-dimensional superstructure characteristic of $Bi_2Sr_2CaCu_2O_x$ superconductors[7,23,24] [Figs. 2(a) and 2(b)]

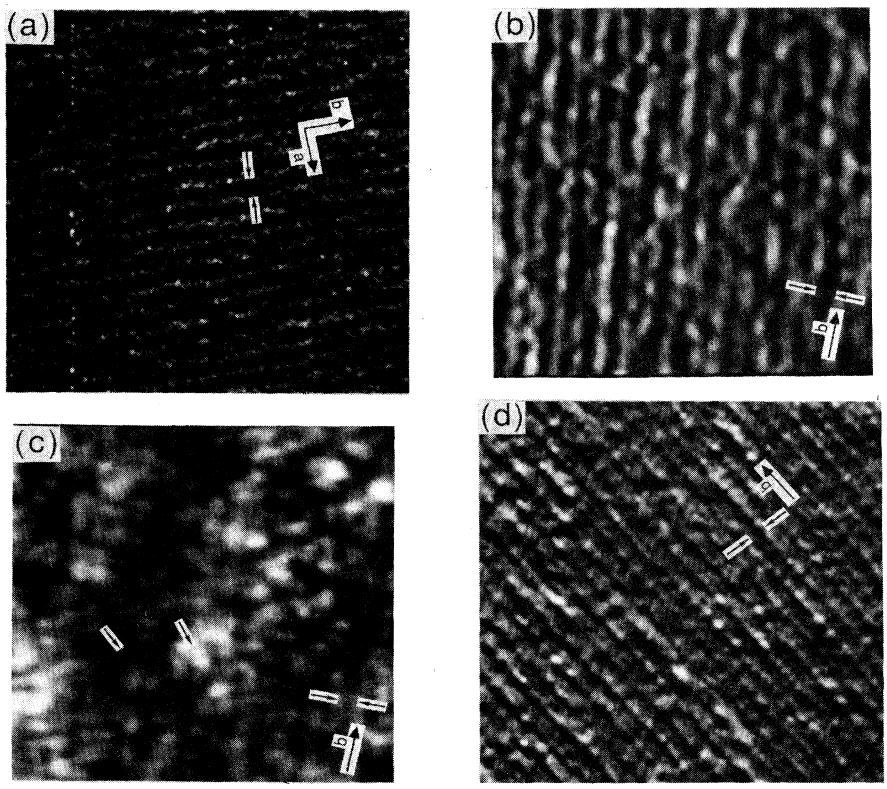

FIG. 2. Grey-scale STM images of (a) $T_c = 85$-K, (b),(c) nonsuperconducting, and (d) reannealed superconducting samples recorded with bias voltages (tunneling currents) of 200 (0.6), 900 (1.5), 150 (1.5), and 150 mV (2.0 nA), respectively. The a,b tetragonal cell axes are shown in (a); the b axis marked in (b) and (c) highlights the same superstructure maxima in both images. Two small arrows in (a)–(d) mark adjacent maxima of the superstructure modulation which are separated by ≈ 25 Å. Two of the irregular electronic features detected at low V_b in the nonsuperconducting samples are highlighted by additional arrows in (c). Magnetic measurements made on the nonsuperconducting samples after imaging showed that these materials remained nonsuperconducting for our experimental conditions. Images (a) and (d) are 500×500 Å^2, and (b) and (c) are 450×450 Å^2.

with nearly the same period: 24.9 ± 1.5 and 26 ± 1 Å, respectively. The small increase in average superstructure period for the nonsuperconducting samples is consistent with models suggesting that extra oxygen in the BiO layer causes this structural modulation.[7,8,23–25] The uncertainty in our data is too large, however, to determine conclusively whether this increase is due to the oxygen removed from these crystals.

Significant changes in the images of the nonsuperconducting materials are observed with variations in V_b. Specifically, while the image of the nonsuperconducting material recorded with $V_b = 900$ mV exhibits a similar superstructure as $T_c = 85$-K samples, an image acquired with $V_b = 150$ mV exhibits new nonperiodic features in addition to a contribution from the superstructure [Fig. 2(c)]; the apparent vertical corrugation of the nonperiodic features is ~ 5 times larger than the superstructure amplitude and dominates the low V_b image. The images of the oxygen-deficient samples, Figs. 2(b) and 2(c), were recorded simultaneously by switching V_b between 900 and 150 mV on alternate scan lines, and thus these images correspond to same area of the surface. Analysis of these data shows that the observed superstructure has the same spatial location in both the high and the low V_b images as is expected for a true structural feature. Extensive imaging studies also show that the STM topographs exhibit the new nonperiodic features between -300 and $+500$ mV, but for $V_b < -500$ and $V_b > 700$ mV only the regular superstructure characteristic of the $T_c = 85$-K material is observed. These significant V_b-dependent changes observed in images of the nonsuperconducting materials are reversible. Nonsuperconducting samples annealed at 400 °C in air for ≥ 8 h, which incorporates the oxygen removed by vacuum annealing, are superconducting ($T_c \approx 85$ K, Fig. 1), and images of these reannealed samples [Fig. 2(d)] are similar to images of as grown $T_c = 85$-K crystals [Fig. 2(a)].

These V_b-dependent data provide significant insight into the local effects of oxygen loss in the nonsuperconducting materials. First, the observation of the superstructure in the same spatial location at both low and high V_b [Figs. 2(b) and 2(c)] is strong evidence that the observed superstructure corresponds to a structural modulation in the BiO layer and not to an electronic effect.[26] However, the fact that the irregular features in images of the nonsuperconducting samples are observed only at low V_b indicates that these features are due to variations in the electronic states near the Fermi level. These irregular electronic features are not observed in images of $T_c = 85$-K samples at low or high V_b, and thus we conclude that these features reflect variations in the electronic structure due to oxygen loss. It is apparent from this work that STM can be used to assess spatial variations in the electronic properties of $Bi_2Sr_2CaCu_2O_x$ due to oxygen doping. Importantly, these variations occur on the same scale (20–30 Å) as the coherence length, and thus they would be expected to affect pairing in intermediate doped crystals. The large-area V_b-dependent images (e.g., Fig. 2) cannot be used, however, to determine the structural sites from which oxygen is removed.

Previous studies have suggested that oxygen doping in $Bi_2Sr_2CaCu_2O_x$ occurs through loss or gain of oxygen in the BiO layers.[9,12–15,23] Since the BiO layer is directly imaged in the STM experiment we have recorded atomic-resolution images to investigate the structural details of oxygen loss from our samples. Images of oxygen deficient nonsuperconducting and $T_c \approx 85$-K crystals exhibit similar atomic structure (Fig. 3). The images of the BiO layer of the oxygen-deficient crystals do not exhibit vacancies or strongly perturbed sites. Our thermogravimetric analysis results indicate that we should have observed an $\sim 2\%$ level of defects if all of the oxygen was removed from the BiO layers. This suggests that oxygen is not removed from the BiO layer since 2% defects are detectable (but not observed) with our STM. It is uncertain, however, whether the atomic structure (period ≈ 3.8 Å) corresponds to the Bi or oxygen lattice sites,[10,16–19,27] and thus we are unable to conclude from this data that oxygen is not lost from the BiO layer. For example, if the Bi sites are imaged, then variations in oxygen content of the BiO layer (accommodated by changes in Bi coordination[8]) will not yield localized structural defects but will vary the density of electronic states. Alternatively, it is possible that oxygen is lost from the SrO or CuO layers. To distinguish these possibilities in the future will require images that simultaneously resolve both Bi and O lattice sites.

Regardless of the sites from which oxygen is lost, these studies do demonstrate that V_b-dependent STM imaging can be used to characterize spatial variations in the elec-

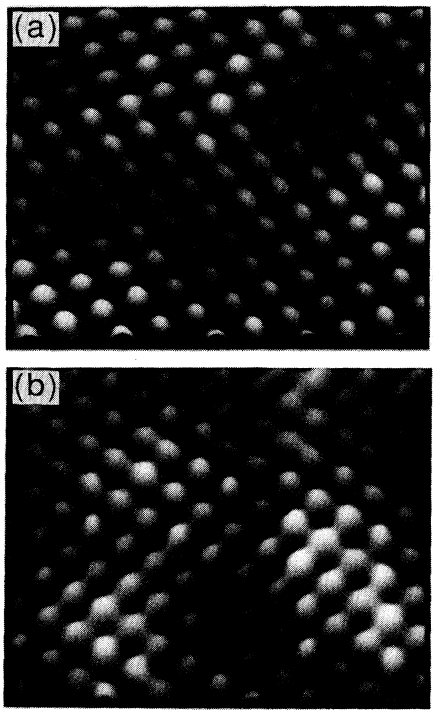

FIG. 3. 40×40 Å^2 perspective view images of (a) superconducting and (b) nonsuperconducting crystals recorded with bias voltages (tunneling currents) of 200 (1.0) and 275 mV (1.2 nA), respectively. The atomic lattice in both images is tetragonal with an average spacing of 3.8 Å between the lattice sites.

tronic states due to oxygen doping. We believe that our results are especially important since these electronic variations occur on the same length scale as the coherence of the superconducting pairs. In the future there are a number of critical issues that should be addressed. For example, it will be important to assess how the spatial variations in the normal-state electronic properties correlate with variations in the superconducting energy gap, and to determine whether the random electronic features observed in intermediate doped crystals order with annealing time. Such studies should significantly further our understanding of the relationship between oxygen doping, local electronic structure, and superconductivity in this system.

We thank R. Feenstra and C. K. Shih for communication of their results prior to publication. C.M.L. acknowledges support of this work by the David and Lucile Packard, A. P. Sloan, and National Science Foundations.

[1]R. J. Cava, Science **247**, 656 (1990).
[2]M. Daeumling, J. M. Seuntjens, and D. C. Larbalestier, Nature (London) **346**, 332 (1990).
[3]J. D. Jorgensen, S. Pei, P. Lightfoot, H. Shi, A. P. Paulikas, and B. W. Veal, Physica C **167**, 571 (1990).
[4]B. W. Veal, H. You, A. P. Paulikas, H. Shi, Y. Fang, and J. W. Downey, Phys. Rev. B **42**, 4770 (1990).
[5]A. Maignan, C. Martin, M. Huve, J. Provost, M. Hervieu, C. Michel, and B. Raveau, Physica C **170**, 350 (1990).
[6]R. J. Cava, Nature (London) **346**, 110 (1990).
[7]P. Bordet, J. J. Capponi, C. Chaillout, J. Chenavas, A. W. Hewat, E. A. Hewat, J. L. Hodeau, and M. Marezio, Stud. High Temp. Supercond. **2**, 171 (1989).
[8]A. Yamamoto, M. Onoda, E. Takayama-Muromachi, F. Izumi, T. Ishigaki, and H. Asano, Phys. Rev. B **42**, 4228 (1990).
[9]L. Forro, J. R. Cooper, B. Leontic, and B. Keszei, Europhys. Lett. **10**, 371 (1989).
[10]Z. Zhang, Y. L. Wang, X. L. Wu, J. L. Huang, and C. M. Lieber, in Proceedings of the Second World Congress on Superconductivity, Houston, 1990 (unpublished).
[11]M. F. Crommie and A. Zettl, Phys. Rev. B **41**, 10978 (1990).
[12]H. M. O'Bryan, W. W. Rhodes, and P. K. Gallagher, Chem. Mater. **2**, 421 (1990).
[13]W. A. Groen and D. M. de Leeuw, Physica C **159**, 417 (1989).
[14]R. G. Buckley, J. L. Tallon, I. W. M. Brown, M. R. Presland, N. E. Flower, P. W. Gilberd, M. Bowden, and N. B. Milestone, Physica C **156**, 629 (1988).
[15]J. M. Tarascon, Y. Le Page, P. Barboux, B. G. Bagley, L. H. Greene, W. R. McKinnon, G. W. Hull, M. Giroud, and D. M. Hwang, Phys. Rev. B **37**, 9382 (1988).
[16]X. L. Wu, Z. Zhang, Y. L. Wang, and C. M. Lieber, Science **248**, 1211 (1990).
[17]S. P. Kelty and C. M. Lieber, Phys. Rev. B **40**, 5856 (1989).
[18]M. D. Kirk, J. Nogami, A. A. Baski, D. B. Mitzi, A. Kapitulnik, T. H. Geballe, and C. F. Quate, Science **242**, 1673 (1988).
[19]C. K. Shih, R. M. Feenstra, J. R. Kirtley, and G. V. Chandrashekhar, Phys. Rev. B **40**, 2682 (1989).
[20]B. O. Wells, Z.-X. Shen, D. S. Dessau, W. E. Spicer, C. G. Olson, D. B. Mitzi, A. Kapitulnik, R. S. List, and A. Arko, Phys. Rev. Lett. **65**, 3056 (1990).
[21]J. M. Imer, F. Patthey, B. Dardel, W. D. Schneider, Y. Baer, Y. Petroff, and A. Zettl, Phys. Rev. Lett. **62**, 336 (1989).
[22]J. E. Demuth, B. N. J. Persson, F. Holtzberg, and C. V. Chandrasekhar, Phys. Rev. Lett. **64**, 603 (1990); B. N. J. Persson and J. E. Demuth, Phys. Rev. B **42**, 8057 (1990).
[23]H. W. Zandbergen, W. A. Groen, F. C. Mijlhoff, G. van Tendeloo, and S. Amelinckx, Physica C **156**, 325 (1988).
[24]Y. Le Page, W. R. McKinnon, J. M. Tarascon, and P. Barboux, Phys. Rev. B **40**, 6810 (1989).
[25]Based on the quantitative analysis of the oxygen deficiency, in the nonsuperconducting versus superconducting crystals (2.5–3%), the superstructure period would be expected to increase about 0.6–0.7 Å.
[26]R. J. Hamers, Annu. Rev. Phys. Chem. **40**, 531 (1989).
[27]C. K. Shih, R. M. Feenstra, and G. V. Chandrashekhar (unpublished).

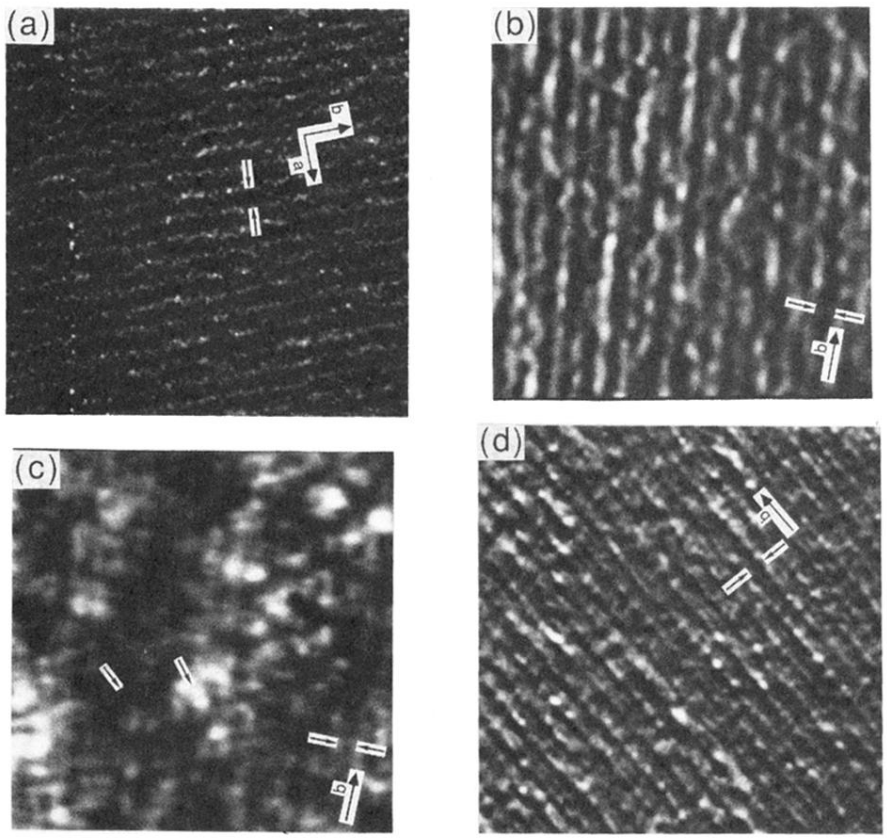

FIG. 2. Grey-scale STM images of (a) $T_c = 85$-K, (b),(c) nonsuperconducting, and (d) reannealed superconducting samples recorded with bias voltages (tunneling currents) of 200 (0.6), 900 (1.5), 150 (1.5), and 150 mV (2.0 nA), respectively. The a,b tetragonal cell axes are shown in (a); the b axis marked in (b) and (c) highlights the same superstructure maxima in both images. Two small arrows in (a)–(d) mark adjacent maxima of the superstructure modulation which are separated by ≈ 25 Å. Two of the irregular electronic features detected at low V_b in the nonsuperconducting samples are highlighted by additional arrows in (c). Magnetic measurements made on the nonsuperconducting samples after imaging showed that these materials remained nonsuperconducting for our experimental conditions. Images (a) and (d) are 500×500 Å^2, and (b) and (c) are 450×450 Å^2.

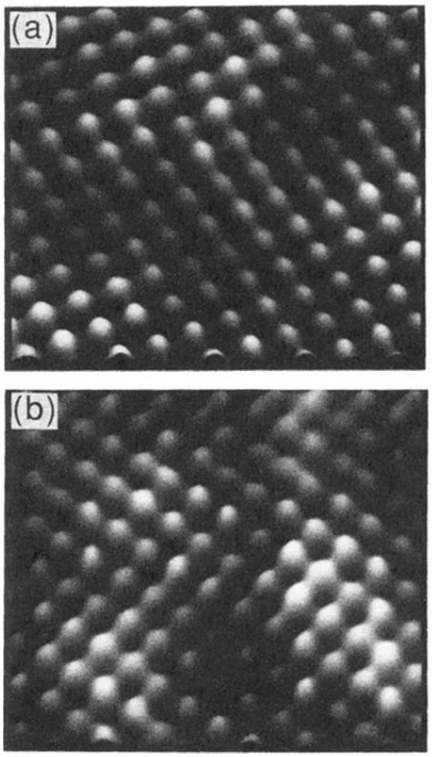

FIG. 3. 40×40 Å^2 perspective view images of (a) superconducting and (b) nonsuperconducting crystals recorded with bias voltages (tunneling currents) of 200 (1.0) and 275 mV (1.2 nA), respectively. The atomic lattice in both images is tetragonal with an average spacing of 3.8 Å between the lattice sites.